

## U2 snRNA-Protein Contacts in Purified Human 17S U2 snRNPs and in Spliceosomal A and B Complexes

Olexandr Dybkov, Cindy L. Will, Jochen Deckert, Nastaran Behzadnia, Klaus Hartmuth, and Reinhard Lührmann\*

*Department of Cellular Biochemistry, Max Planck Institute for Biophysical Chemistry, D-37077 Göttingen, Germany*

Received 28 November 2005/Returned for modification 23 December 2005/Accepted 13 January 2006

**The 17S U2 snRNP plays an essential role in branch point selection and catalysis during pre-mRNA splicing. Much remains to be learned about the molecular architecture of the U2 snRNP, including which proteins contact the functionally important 5' end of the U2 snRNA. Here, RNA-protein interactions within immunoaffinity-purified human 17S U2 snRNPs were analyzed by lead(II)-induced RNA cleavage and UV cross-linking. Contacts between the U2 snRNA and SF3a60, SF3b49, SF3b14a/p14 and SmG and SmB were detected. SF3b49 appears to make multiple contacts, interacting with the 5' end of U2 and nucleotides in loops I and IIb. SF3a60 also contacted different regions of the U2 snRNA, including the base of stem-loop I and a bulge in stem-loop III. Consistent with it contacting the pre-mRNA branch point adenosine, SF3b14a/p14 interacted with the U2 snRNA near the region that base pairs with the branch point sequence. A comparison of U2 cross-linking patterns obtained with 17S U2 snRNP versus purified spliceosomal A and B complexes revealed that RNA-protein interactions with stem-loop I and the branch site-interacting region of U2 are dynamic. These studies provide important insights into the molecular architecture of 17S U2 snRNPs and reveal U2 snRNP remodeling events during spliceosome assembly.**

Pre-mRNA splicing is catalyzed by the spliceosome, a large dynamic macromolecular machinery, which assembles by the highly coordinated, sequential association of four small nuclear RNPs (snRNPs) and a large number of non-snRNP protein splicing factors with conserved sequences of the pre-mRNA (reviewed in reference 51). A number of spliceosome assembly intermediates can be detected *in vitro* by biochemical means. First, U1 snRNP interacts with the 5' splice site to form the spliceosomal E (early) complex. The U2 snRNP is weakly associated with this complex (9), and subsequently it stably interacts with the branch point sequence (BPS) of the pre-mRNA in an ATP-dependent fashion, forming complex A. In the next step the U4/U6.U5 tri-snRNP is incorporated into the spliceosome, generating complex B. Significant RNA and protein rearrangements, which lead to destabilization (or release) of the U1 and U4 snRNPs, generate the catalytically activated spliceosome (B\*) (reviewed in reference 41). The subsequent catalytic steps of splicing involve two sequential transesterification reactions (reviewed in reference 51). In the first step, the branch point adenosine carries out a nucleophilic attack at the 5' splice site, which generates the cleaved 5' exon and intron 3' exon. In the second, the 3' splice site is cleaved, resulting in the excision of the intron and ligation of the 5' and 3' exons. The spliced-out intron is subsequently degraded, and the snRNPs are released to participate in new rounds of splicing.

The U2 snRNP plays a pivotal role in splicing. It participates in proper selection and subsequent positioning of the branch point adenosine (the nucleophile for the first catalytic step)

within the catalytic core of the spliceosome. The U2 snRNA first establishes a short duplex with the BPS of the intron, in which the branch adenosine is bulged out (reference 35 and references therein). It then forms several short duplexes with the U6 snRNA (e.g., helices I, II, and III) (19, 27, 42). Together with U6, which also base pairs with the 5' splice site, U2 forms part of the RNA network that brings into close proximity the reactive sites of the pre-mRNA and is thus at the catalytic core of the spliceosome (reviewed in reference 31).

The human U2 snRNP, which consists of the U2 snRNA and several proteins, has a modular structure. It was first described as a 12S particle that consists of the seven Sm proteins, common to all but the U6 and U6atac spliceosomal snRNPs, and two U2-specific proteins A' and B" (reviewed in reference 50). The splicing-active 17S U2 snRNP additionally contains the heteromeric splicing factors SF3a and SF3b (2); they consist of three proteins (SF3a120, SF3a66, and SF3a60) and seven proteins (SF3b155, SF3b145, SF3b130, SF3b49, SF3b14a/p14, SF3b14b, and SF3b10), respectively (8, 15, 25, 53, 55). SF3a and SF3b are required for A complex formation (3) and contribute to the selection of the BPS by stabilizing the U2 snRNP-BPS interaction. Components of SF3a and SF3b interact either directly with the branch adenosine (i.e., SF3b14a/p14) or with a region ~25 nucleotides (nt) upstream or 5 nt downstream of the BPS (15, 16, 53). Due to their close proximity to the branch adenosine, several SF3b proteins are likely to be core components of the spliceosome. Orthologues of nearly all SF3a and SF3b components have also been identified in the yeast *Saccharomyces cerevisiae* (5, 12, 22, 47). More recently, a number of other proteins were found to associate with the human 17S U2 snRNP, the majority of which are present in substoichiometric amounts (55).

Although a great deal has been learned about the organization of components of the U2 snRNP, a complete picture of its

\* Corresponding author. Mailing address: Department of Cellular Biochemistry, Max Planck Institute for Biophysical Chemistry, Am Fassberg 11, 37077 Göttingen, Germany. Phone: 49-551-2011407. Fax: 49-551-2011197. E-mail: Reinhard.Luehrmann@mpi-bpc.mpg.de.

molecular architecture is currently missing. The core RNP structure of the U2 snRNP consists of the seven Sm proteins G, F, E, D1, D2, D3, and B/B' that interact with the conserved Sm site of the U2 snRNA to form a seven-membered ring, the inner surface of which contacts the Sm site (23, 45). The majority of U2-specific proteins, including SF3a, SF3b, and U2-B''/U2-A', form stable heteromeric complexes in the absence of the U2 snRNA. Currently only the U2-B''/U2-A' heterodimer has been shown to directly bind the U2 snRNA, specifically recognizing stem-loop IV (SLIV) (reviewed in reference 46). The atomic structure of the human U2-B''/U2-A' heterodimer complexed with an RNA hairpin comprising U2 SLIV was determined previously (33).

Recently the three-dimensional structure of purified human SF3b, the largest U2 subunit, was obtained by single-particle electron microscopy (13). The relative orientations of several SF3b proteins and their domains could be determined. In particular, the SF3b155 C-terminal HEAT repeats are located on the outer shell of SF3b and curve around the entire complex, whereas the two RRM of SF3b49 are found on the periphery and the SF3b14a/p14 RRM is localized in the central cavity. As SF3b14a/p14 was shown to directly interact with the branch point adenosine of pre-mRNA upon stable incorporation of U2 into the spliceosome (36, 53), SF3b likely undergoes a dramatic conformational change either upon integration into the U2 snRNP or during U2 association with the pre-mRNA. The former is supported by a recent electron cryomicroscopy study of the U11/U12 di-snRNP. U11 and U12 are the functional counterparts of U1 and U2, respectively, in the minor U12-type spliceosome that is responsible for splicing a rare class of pre-mRNA introns (reviewed in reference 32). SF3b also associates with the U11/U12 di-snRNP (54), and it is found in a more open conformation in this particle compared to isolated SF3b (14).

Several protein-protein interactions within the SF3a and SF3b complexes are well documented, including highly stable interactions between SF3b155 and SF3b14a/p14 (53), SF3b145 and SF3b49 (6), SF3a120 and SF3a60 (7), and SF3a120 and SF3a66 (24). However, relatively little is known about how these functionally important complexes are tethered to the U2 snRNP. Electron microscopy studies suggest that the 17S U2 snRNP consists of two 10- to 12-nm globular domains, of which one contains SF3b and a 5' portion of the U2 snRNA whereas the other contains the Sm core, U2-B''/U2-A', SF3a, and the 3' part of the U2 snRNA (2, 25).

Here, we have investigated RNA-protein interactions within the human 17S U2 snRNP. Native human 17S U2 snRNPs, immunoaffinity purified from HeLa nuclear extract, were analyzed by RNA cleavage with lead(II) and UV-induced cross-linking followed by immunoprecipitation and primer extension analyses. Data from these studies revealed contacts between the U2 snRNA and SF3a60, SF3b49, and SF3b14a/p14. UV cross-linking studies with *in vitro*-reconstituted U2 snRNPs confirmed an interaction between SF3b49 and the extreme 5' end of the U2 snRNA. Subsequent UV cross-linking with affinity-purified spliceosomal A and B complexes revealed remodeling events involving RNA-protein contacts at the 5' end of the U2 snRNA upon stable incorporation of the U2 snRNP into the A complex. Our data thus provide important insight into the molecular architecture of the 17S U2 snRNP and

reveal that the U2 snRNP is partially remodeled during spliceosome assembly.

## MATERIALS AND METHODS

**Antibodies.** The following rabbit polyclonal antibodies were used in this study: anti-SF3a120 (directed against a peptide comprising amino acids [aa] 437 to 451) (53), anti-SF3b155 (aa 99 to 113) (53), anti-SF3b14a/p14 (aa 111 to 125) (53), anti-SF3a66 (aa 444 to 458) (55) and anti-G (raised against a glutathione *S*-transferase-SmG fusion protein) (21). Rabbit anti-SF3a60, anti-SF3b145, and anti-SF3b49 antibodies and mouse anti-SF3a120 monoclonal antibodies were generated against peptides DYTRVVKPLODQNEL, AMTKYEEHVREQQA, MAAGPISERNQDATV, and RWLEQRDRSIREKQS (encompassing aa 195 to 209, 816 to 830, 1 to 15, and 437 to 451, respectively). The mouse monoclonal antibody Ana125 was used to precipitate SmB/B' (34). Rabbit antibodies were affinity purified as described previously (55) and reacted specifically with the corresponding protein on immunoblots containing HeLa nuclear extract proteins (data not shown).

**Purification of the human 17S U2 snRNP.** HeLa cell nuclear extract was prepared according to the method described in reference 10 and dialyzed against G150 buffer (20 mM HEPES-KOH, 150 mM KCl, 1.5 mM MgCl<sub>2</sub>, 5% glycerol, 0.5 mM dithioerythritol, 0.5 mM phenylmethylsulfonyl fluoride, pH 7.9). It was then diluted with an equal volume of the same buffer and centrifuged at 15,000 × *g* for 10 min to remove precipitates. The supernatant was passed over an immunoaffinity chromatography column containing monoclonal mouse anti-peptide antibodies directed against the SF3a120 protein or polyclonal rabbit anti-peptide antibodies against the SF3a66 protein (55), covalently coupled to protein G- or A-Sepharose with dimethylpimelimidate, respectively (52). After extensive washes, 17S U2 snRNPs were eluted from the column with 3 column volumes of G150 buffer containing 0.4 mg/ml of the cognate peptide. Purified U2 snRNPs were fractionated on a 10% to 30% glycerol gradient as described previously (55). The RNA and protein components of the U2 snRNP were analyzed by denaturing gel electrophoresis and sodium dodecyl sulfate-polyacrylamide gel electrophoresis (SDS-PAGE), respectively.

***In vitro* reconstitution of 17S U2 snRNPs.** Reconstitution of 17S U2 snRNPs was performed as described previously (11, 38). Briefly, chimeric U2 snRNA was prepared by ligation of a synthetic oligoribonucleotide comprising U2 nt 1 to 24 to *in vitro*-transcribed U2 snRNA encompassing nt 25 to 187 (29). RNAs were then incubated with native, purified total snRNP proteins *in vitro* and subsequently with HeLa nuclear extract depleted of endogenous 12S U2 snRNPs.

**Purification of human spliceosomal A and B complexes.** Spliceosomal A and B complexes formed on MINX pre-mRNA were purified from splicing reactions by using the previously described tobramycin affinity selection method (18). Briefly, MINX pre-mRNA containing the J6f1 tobramycin binding RNA aptamer was first bound to tobramycin covalently coupled to Sepharose and then incubated with HeLa nuclear extract under splicing conditions for 45 min. Following several wash steps, complexes were eluted from the matrix by incubation with 5 mM tobramycin. A and B complexes were separated by centrifugation at 374,000 × *g* for 107 min in a TH660 rotor (Sorvall), using a linear 10% to 30% (vol/vol) glycerol gradient, which was fractionated manually from the top. Fractions 11 to 12 and 15 to 16 were enriched in complexes A and B, respectively. Additionally, complex B was assembled on a pre-mRNA tagged with three MS2-binding sites and purified via the MS2-MBP affinity purification method (9). Briefly, MINX pre-mRNA was prebound with the MS2-MBP fusion protein and spliceosomes were allowed to form by performing splicing in HeLa nuclear extract for 8 min. Spliceosomal complexes were fractionated by gradient centrifugation on 10%-to-30% (vol/vol) glycerol gradients (in 20 mM HEPES-KOH [pH 7.9], 1.5 mM MgCl<sub>2</sub>, 150 mM NaCl) in a Centrikon TST 41.14 rotor for 16 h at 80,000 × *g*, and gradient fractions were harvested manually from the top. Peak gradient fractions containing spliceosomal B complex were pooled and applied to amylose beads (NEB) preequilibrated with 20 mM HEPES-KOH (pH 7.9), 150 mM NaCl, and 1.5 mM MgCl<sub>2</sub>. Amylose beads were then washed with 15 column volumes of preequilibration buffer, and bound spliceosomal B complexes were eluted with preequilibration buffer containing 12 mM maltose. RNA was recovered from the purified complexes by extraction with phenol:chloroform:isoamylalcohol (PCI), analyzed on a 7 M urea-10% polyacrylamide gel, and visualized by staining with silver.

**Lead(II)-induced U2 snRNA cleavage.** 17S U2 snRNPs, and U2 snRNA extracted from 17S U2 particles with PCI at 4°C, were dialyzed against buffer N1 (20 mM HEPES-NaOH, 5 mM magnesium acetate, 100 mM potassium acetate, pH 7.5). RNA cleavage was induced by addition of 5 to 45 mM lead(II) acetate and subsequent incubation for 5 min at 20°C (4). Reactions were terminated by addition of 50 mM EDTA. Samples were precipitated with ethanol, dissolved in

PK buffer (100 mM Tris-HCl, 150 mM NaCl, 12.5 mM EDTA, 1% SDS, pH 7.5), and incubated with 1 mg/ml proteinase K for 1 h at 42°C. Following phenol-chloroform extraction, RNAs were precipitated twice with ethanol. The RNA was dissolved in CE buffer (20 mM cacodylic acid-KOH, 0.2 mM EDTA, pH 7.0), and RNA cleavage sites were analyzed by primer extension.

**UV cross-linking of 17S U2 snRNPs, spliceosomal A and B complexes, and naked U2 snRNA.** Approximately 14 pmol of immunoaffinity-purified 17S U2 snRNPs or purified spliceosomal A and B complexes was pipetted in a thin layer into a 24-well microtiter plate and then subjected to 254 nm UV irradiation for 30 to 120 s on ice essentially as described previously (44). In parallel, U2 snRNA that had been extracted with PCI from approximately 2 pmol of 17S U2 snRNPs or spliceosomal complexes at 4°C was cross-linked under the same conditions. Irradiated and nonirradiated control samples of U2 snRNP and U2 RNA were precipitated with 3 volumes of ethanol in the presence of 0.3 M sodium acetate, pH 5.2. The pellets were dissolved in 25  $\mu$ l of 20 mM sodium phosphate buffer containing 130 mM NaCl (PBS; pH 8.0) supplemented with 3% SDS, incubated for 2 min at 96°C followed by 10 min at 70°C, and allowed to cool to room temperature. Triton X-100 was added to a final concentration of 5%. The volume was adjusted to 375  $\mu$ l with PBS containing 0.5 mM dithioerythritol. Prior to primer extension analysis, 12 pmol of the sample was subjected to immunoprecipitation (see below) and 2 pmol was directly digested with proteinase K, extracted with PCI, precipitated twice with ethanol, and dissolved in CE buffer.

**Immunoprecipitation of RNA-protein cross-links.** Polyclonal rabbit antibodies directed against a given U2 snRNP-specific protein were bound to protein A-Sepharose beads. After being washed with PBS, the antibody-bound beads were incubated with PBS containing 50  $\mu$ g/ml yeast tRNA, 0.5 mg/ml bovine serum albumin, and 0.01% NP-40 for 2 h. Beads were subsequently washed three times with PBS and incubated for 1 h at 4°C with UV cross-linked or non-cross-linked 17S U2 snRNPs that had been disrupted by heating at 96°C in the presence of 3% SDS (see above). After being washed extensively with PBS, beads were incubated with 2 $\times$  PK buffer for 5 min at 95°C and then diluted with an equal volume of water. Proteins were digested on the beads with proteinase K (end concentration of 0.5 mg/ml) for 1 h at 42°C. The RNA and peptide-RNA cross-linked species were extracted with PCI, precipitated twice with ethanol, and dissolved in CE buffer.

**Primer extension analysis.** Oligodeoxynucleotide primers complementary to positions 77 to 97 (k91), 97 to 117 (J1), or 149 to 169 (k31) of the human U2 snRNA were <sup>32</sup>P labeled at their 5' end by use of T4 polynucleotide kinase, and ~1 to 2  $\times$  10<sup>5</sup> cpm of primer was added to U2 snRNA-containing samples. The samples were denatured by heating at 96°C for 1 min, allowed to anneal by cooling to room temperature, and reverse transcribed with 1.5 U of AMV reverse transcriptase (USB) per reaction for 50 min at 42.5°C. Sequencing ladders were obtained from in vitro-transcribed U2 RNA under identical conditions except that 0.5 mM dideoxynucleoside triphosphates were added. Reverse transcripts were separated on an 8.3 M urea-9.6% polyacrylamide sequencing gel and visualized by autoradiography.

## RESULTS

To learn more about the molecular architecture of the 17S U2 snRNP, we examined RNA-protein interactions within this particle by lead(II) cleavage footprinting and direct UV cross-linking. For this purpose, native human 17S U2 snRNPs were immunoaffinity-purified from HeLa nuclear extract using anti-SF3a120 monoclonal antibodies bound to protein G-Sepharose. Particles were eluted under native conditions with an excess of cognate peptide, and their RNA and protein compositions were analyzed. As shown in Fig. 1, highly pure U2 snRNPs could be isolated, as evidenced by the presence of almost exclusively U2 snRNA in the eluate (Fig. 1A), and they possess the same protein composition—as evidenced by SDS-PAGE (Fig. 1B) and mass spectrometry (not shown)—as human 17S U2 snRNPs previously immunoaffinity purified with anti-SF3a66 antibodies (55). Importantly, immunoaffinity-purified 17S U2 snRNPs exhibited a homogeneous sedimentation behavior during glycerol gradient centrifugation, with nearly all particles sedimenting in fractions 13 to 15 (Fig. 1C), which correspond to the 17S region of the gradient.

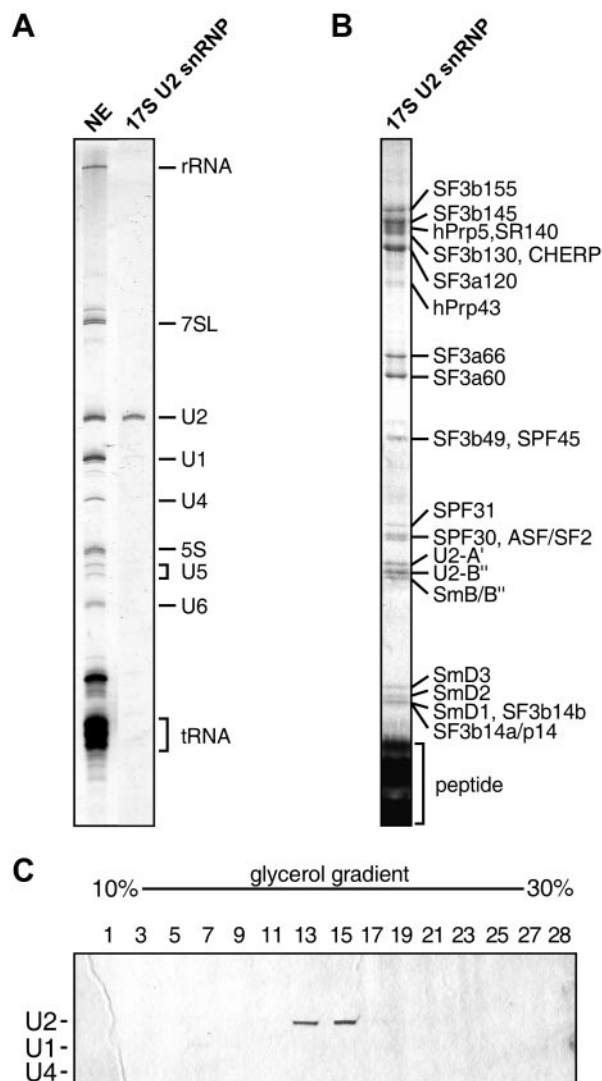


FIG. 1. Characterization of immunoaffinity-purified human 17S U2 snRNPs. (A and B) The RNA (A) and protein (B) compositions of 17S U2 snRNPs immunoaffinity purified with antibodies against SF3a120 were analyzed by denaturing and SDS-PAGE, respectively. RNA was visualized by silver staining and protein by staining with Coomassie blue. The identity of RNA or protein is shown on the right. NE, nuclear extract. (C) Purified 17S U2 snRNPs were fractionated on a 10% to 30% glycerol gradient, and the RNA composition of odd-numbered and bottom gradient fractions (as indicated above) was determined as described for panel A.

**Lead(II)-induced cleavage of U2 snRNA.** Previous structure probing of the human 17S U2 snRNP was limited to chemical probing with DMS and kethoxal (2). To obtain more information about the secondary structure of the U2 snRNA and those nucleotides that might be involved in RNA-protein interactions within the 17S U2 snRNP, we compared the lead(II)-induced RNA cleavage pattern of naked U2 snRNA and U2 snRNA within native 17S U2 particles. Lead(II) cations induce cleavages of RNA molecules in single-stranded and bulged regions that are not spatially constrained or protected by proteins (4). The reactivity of the sugar-phosphate backbone of naked U2 snRNA towards lead(II), as determined by reverse

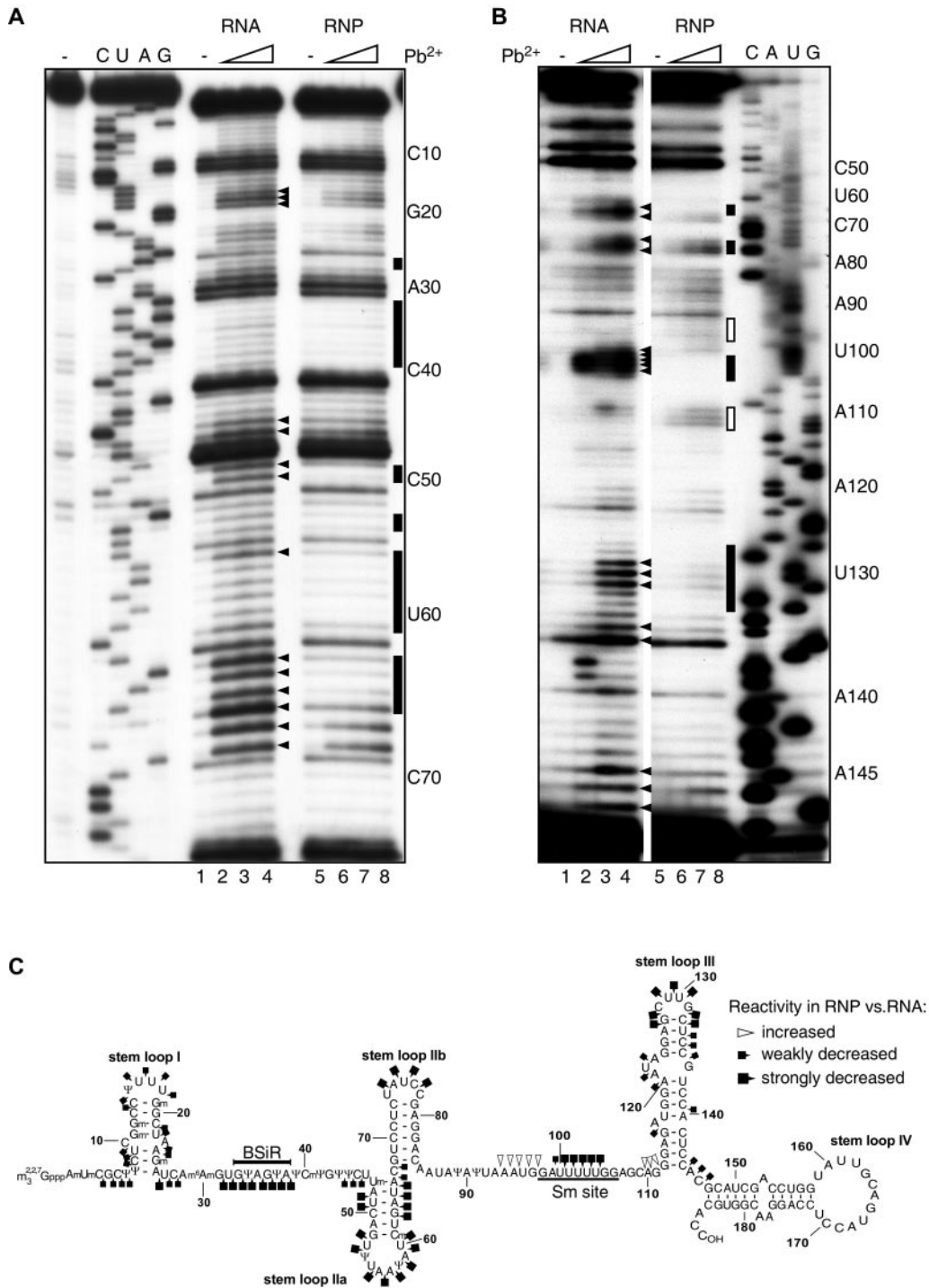


FIG. 2. Lead(II)-induced cleavage of native human 17S U2 snRNPs. (A and B) Isolated U2 snRNA (RNA; lanes 1 to 4) or immunoaffinity-purified 17S U2 snRNP (RNP; lanes 5 to 8) was probed with increasing concentrations of lead(II) acetate (0, 5, 15, and 45 mM; lanes 1 to 4 and 5 to 8). Cleavage sites were assayed by primer extension using oligonucleotides complementary to nt 97 to 117 (A) or 149 to 169 (B) and were visualized by autoradiography. A sequencing ladder (on the left or right) was obtained by primer extension of in vitro-transcribed U2 RNA in the presence of dideoxynucleotides. Those nucleotides that are strongly cleaved in the naked RNA are indicated by arrows to the right of lane 4. Regions of U2 snRNA with increased or strongly reduced reactivity towards lead(II) when probed in the 17S U2 snRNP are marked by an open or closed bar, respectively. Positions of the nucleotides are shown on the right of each panel. (C) Schematic representation of the comparative reactivity of U2 snRNA in the purified 17S U2 snRNP versus isolated U2 snRNA. Increased reactivity towards lead(II) of U2 in 17S U2 snRNPs compared to the results seen with isolated U2 snRNA is indicated by open arrowheads and weakly and strongly decreased reactivity by small and large black boxes, respectively. The degree of reactivity was determined by eye by comparing the relative intensity of the bands in the RNA versus RNP lanes, also taking into account the intensity of background in the absence of lead(II). The branch site-interacting region (BSiR) is highlighted by a bar above the corresponding nucleotides, and the Sm site is underlined.

transcription with primers complementary to positions 97 to 117 and 149 to 169 of U2 snRNA, is shown in Fig. 2A and B. Regions efficiently cleaved in the presence of lead(II) (indicated by closed arrows to the right of lane 4 in Fig. 2A and B), as evidenced by greatly enhanced reverse transcription stops (lanes 2 to 4) relative to the control reaction without lead(II) (lane 1), included nucleotides located in (i) the loop of SLI (U17-Gm19) or just upstream of SLIIa (C45-U46), (ii) stem IIa (U49-C50), (iii) the loop of SLIIa (A56), (iv) the region between SLIIa and SLIIB (G63-G68), (v) the loop of SLIIB (A75-C78), (vi) the Sm site (U100-U104), (vii) the loop or bulge of SLIII (U129-G131 and C135-G136), and (viii) a trinucleotide downstream of it (A145-G147). Weakly accessible positions included nucleotides at the 5' end of U2, comprising the stem of SLI, at or near the U2 branch site-interacting region, in loop IIa, at the base of SLIIB and directly downstream of it, and several nucleotides just upstream or within SLIII. The overall cleavage pattern is in good agreement with the previously proposed secondary structure of U2 snRNA (1) (Fig. 2C), as the most reactive sites (with the exception of several nucleotides in the stems of SLIIa and SLIIB) are located in single-stranded regions.

When 17S U2 snRNPs were subjected to lead(II) cleavage, U2 snRNA showed an altered reactivity compared to naked U2 snRNA (Fig. 2A and B, lanes 5 to 8). The comparative analysis of lead(II)-induced cleavage of naked U2 snRNA versus U2 in 17S U2 RNPs is schematically summarized in Fig. 2C. Cleavage of nucleotides in the branch site-interacting region, SLIIa, as well as in loops IIb and III was greatly reduced or even abolished in the case of the Sm site (Fig. 2B; indicated by solid bars to the right of lane 8). Other regions of U2 snRNA weakly reactive in the naked RNA were also less efficiently cleaved in the 17S U2 snRNP, including the 5' end of U2 and SLI. These results suggest either that RNA was directly protected by the presence of proteins in these regions or that its structure was altered (e.g., the formation of base pairs was stabilized) via the interaction with proteins. Interestingly, sequences adjacent to the Sm site (nucleotides 94 to 98 and 110 to 112) were more susceptible to lead(II)-induced cleavage (marked by open bars in Fig. 2B). Taken together, these results suggest that multiple regions of the U2 snRNA are likely contacted by protein in the 17S U2 snRNP.

**Mapping of RNA-protein interaction sites via UV cross-linking.** To more precisely map the RNA-protein interaction sites in native human 17S U2 snRNPs, we performed direct UV cross-linking, followed by immunoprecipitation and primer extension analysis as described previously (44). Exposure to 254-nm UV light is known to induce direct (zero-length) cross-links between nitrogenous bases of nucleic acids and amino acid side chains when they are in a favorable configuration. First we analyzed UV cross-links in native 17S U2 snRNPs purified from HeLa cell nuclear extract ("RNP" lanes), as well as in the naked U2 snRNA ("RNA" lanes) extracted from 17S U2 particles under mild conditions, which should preserve the native secondary structure of the RNA. Putative RNA-protein contact sites were determined by comparing the patterns of reverse transcription (Fig. 3 and 4, lanes 1 to 4). Cross-linked nucleotides interfere with primer extension. Therefore, strong reverse transcriptase stops induced upon UV irradiation that are present in the "RNP" lanes but absent or less intense in

"RNA" lanes should indicate the position of RNA-protein cross-links, with an actual interaction site situated 1 nucleotide upstream from the stop site. In contrast, stops that appear irrespectively of UV irradiation are naturally occurring reverse transcriptase stops and do not result from protein cross-links. For example, major naturally occurring stops were consistently observed at nucleotides 30 to 31, 48, 62, 66, 136, 140, and 145 (Fig. 3 and 4).

A number of putative RNA-protein cross-links could be discerned. Enhanced reverse transcriptase stops were observed at nucleotides C3 and  $\Psi$ 7, in SLI (i.e., at nucleotides U9-Gm11, U16-Gm19, and A23), in the branch point-interacting region (A35 and 38) and just downstream of it ( $\Psi$ 41 and Um47), in SLIIa (U55, A56, and U62), in loop IIb (A75, U76, and C78), upstream of and at the Sm site (A88, A90, U92, A93, U101, and U103), and in SLIII (A123, C128, U130, G131, and C135) (Fig. 3A and B and 4A and B [cf. lanes 1 and 3]; please note that the order of the RNA and RNP lanes is reversed in Fig. 3B). Thus, proteins are potentially cross-linked one nucleotide upstream of these sites in the 17S U2 snRNP (see Fig. 5 for summary). Some of these stops were enhanced in the UV-irradiated versus nonirradiated, naked U2 snRNA (e.g., U17 or A56) (Fig. 3A and 4A [cf. lanes 3 and 4]), and thus they could alternatively represent RNA-RNA cross-links, due to either long-range internal RNA interactions or the formation of pyrimidine dimers. As the most downstream primer that we used annealed to positions 149 to 169, no information about protein-RNA contact sites downstream of C149 was obtained. Taken together, these data indicate that the U2 snRNA is contacted at multiple positions apparently over its entire length by proteins.

**Identification of the protein-RNA cross-links within the U2 snRNA Sm site.** To identify proteins contacting the U2 snRNA, cross-linked RNA-protein species were immunoprecipitated with antibodies against a subset of 17S U2 snRNP proteins, including SmG and SmB, all SF3a subunits (SF3a60, SF3a66, and SF3a120), and several SF3b proteins (i.e., SF3b14a/p14, SF3b49, SF3b145, and SF3b155). These antibodies reacted specifically with their cognate proteins on immunoblots containing HeLa nuclear extract proteins (data not shown). Precipitated cross-links were subsequently identified by primer extension analysis. Prior to immunoprecipitation, 17S U2 snRNPs were disrupted by incubating at 96°C in the presence of 3% SDS (for details, see Materials and Methods). Under these conditions, only SF3b49, SF3b14a/p14, or SF3a60, and no other U2 proteins (as evidenced by silver staining after SDS-PAGE), were precipitated with anti-SF3b49, anti-SF3b14a/p14, or anti-SF3a60 antibodies, respectively, that were covalently coupled to protein A-Sepharose, indicating that the vast majority of U2 snRNPs and their subcomplexes had been dissociated (data not shown). Furthermore, U2 RNA from the nonirradiated U2 snRNP samples was not precipitated by any of the antibodies that were tested (Fig. 3 and 4 and data not shown), further indicating that all non-cross-linked, protein-RNA interactions had been disrupted and also did not reform during immunoprecipitation.

UV irradiation generated at least two RNA-protein cross-links within the Sm site at positions U100 and U102 (Fig. 3B and 4B [cf. lanes 1 and 3]). Primer extension analysis of cross-links immunoprecipitated with anti-SmG antibodies revealed

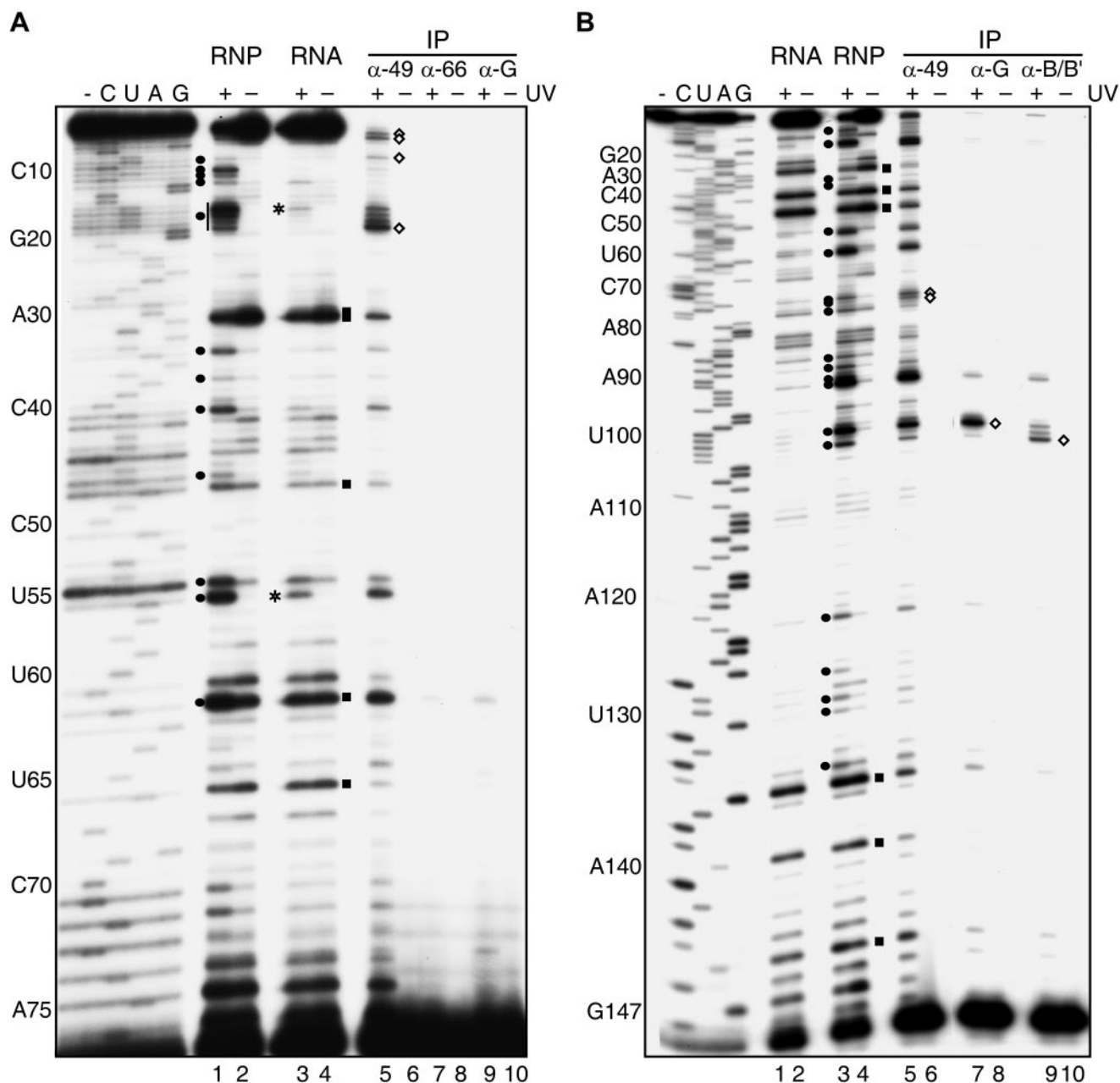


FIG. 3. Identification of UV-induced U2 snRNA-protein cross-linking sites within native human 17S U2 snRNPs. (A) Primer extension analyses of U2 snRNA extracted from UV-irradiated (lane 1) or nonirradiated (lane 2) immunoaffinity-purified 17S U2 snRNPs (RNP) and UV-irradiated (lane 3) or nonirradiated (lane 4) naked U2 snRNA (RNA). (B) Primer extension analyses of UV-irradiated (lane 1) or nonirradiated (lane 2) naked U2 snRNA or U2 snRNA extracted from UV-irradiated (lane 3) or nonirradiated (lane 4) immunoaffinity-purified 17S U2 snRNPs (RNP). Immunoprecipitation (IP) with anti-SF3b49, anti-SmG, anti-SmB/B', or anti-SF3a66 antibodies (as indicated above each lane), followed by primer extension analyses, was performed after denaturation of UV-irradiated (lanes 5, 7, and 9) or nonirradiated (lanes 6, 8, and 10) 17S U2 snRNPs. Primer extension was performed with oligonucleotides complementary to nt 77 to 97 (A) and 149 to 169 (B). Dideoxy sequencing markers were generated as described for Fig. 2. Nucleotide positions are shown on the left. Reverse transcriptase stops due to putative RNA-protein cross-links (closed circles), specific protein-RNA cross-links (open diamonds), potential RNA-RNA cross-links (asterisks), and major background stops (squares) are indicated.

that they precipitated nearly exclusively the cross-link at U100 (i.e., a major reverse transcriptase stop at U101 was observed) (Fig. 3B, lane 7), confirming that SmG contacts this site. Similarly, the cross-link at U102 was highly enriched in the anti-SmB/B' immunoprecipitate, indicating that it is contacted by

SmB/B' (Fig. 3B, lane 9). These data are in accordance with previous UV cross-linking studies performed with a short oligonucleotide derived from the Sm site of the U4 snRNA, which indicated that the first and third residues of the Sm site are contacted by SmG and SmB/B', respectively (45).

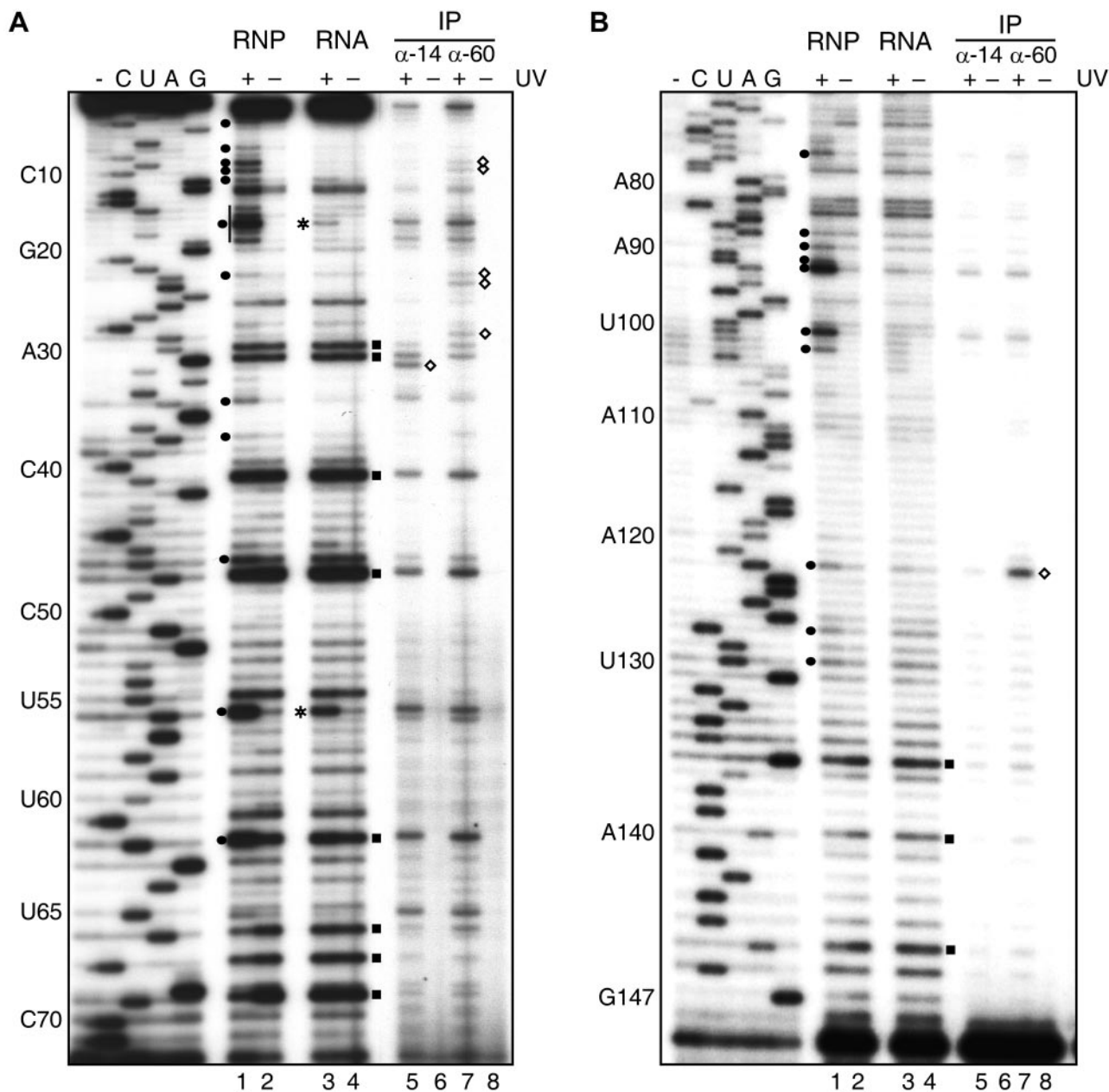


FIG. 4. Identification of protein-RNA contact sites within native human 17S U2 snRNPs. (A and B) Primer extension analyses of U2 snRNA extracted from UV-irradiated (lane 1) or nonirradiated (lane 2) immunoaffinity-purified 17S U2 snRNPs (RNP) and UV-irradiated (lane 3) or nonirradiated (lane 4) naked U2 snRNA (RNA). Immunoprecipitation (IP) with anti-SF3b14a/p14 (lanes 5 to 6) or anti-SF3a60 (lanes 7 to 8) antibodies, followed by primer extension analyses, was performed after denaturation of UV-irradiated (lanes 5 and 7) or nonirradiated (lanes 6 and 8) 17S U2 snRNPs. Primer extension was performed with oligonucleotides complementary to nt 77 to 97 (A) and 149 to 169 (B) and visualized by autoradiography. Dideoxy sequencing markers were generated as described for Fig. 2. Nucleotide positions are shown on the left. Reverse transcriptase stops due to putative RNA-protein cross-links (closed circles), specific protein-RNA cross-links (open diamonds), potential RNA-RNA cross-links (asterisks), and major background stops (squares) are indicated.

**SF3a60 contacts SLI and SLIII of the U2 snRNA.** Anti-SF3a60 antibodies precipitated multiple U2 cross-link species, including some not readily apparent in the input irradiated RNP lane (Fig. 4A and B [cf. lanes 1 and 7]). Several of these, including U16-U18,  $\Psi$ 34,  $\Psi$ 37, U55, Cm61, U92, and U100, were precipitated equally well by other antibodies and were not clearly enriched in the anti-SF3a60 immunoprecipitate (Fig. 3 and 4). Thus, they could not unequivocally be desig-

nated as SF3a60 cross-links. The precipitation of multiple cross-links by several antibodies might be due to cross-linking of two different proteins to the same RNA molecule or arise from incomplete disruption or reassociation of a small fraction of the U2 particles during immunoprecipitation. However, six cross-links were either specifically precipitated by anti-SF3a60 antibodies (i.e., C8-U9 and U22-A23 within SLI as well as C28 downstream of it) or they were significantly enriched relative to



FIG. 5. Summary of U2 snRNA-protein cross-links revealed by immunoprecipitation and primer extension analyses. BSiR, branch site-interacting region.

the input cross-linked material (i.e., U122 in the internal loop of SLIII). All other bands observed by primer extension analysis (e.g., Gm12, m<sup>6</sup>Am30, G31, and Ψ41) represented naturally occurring reverse transcriptase stops. Our results demonstrate that SF3a60 contacts U2 snRNA nucleotides in SLI and SLIII within the U2 snRNP and thus bridges distant regions of the RNA molecule (see Fig. 5 for a summary of cross-links).

In contrast, U2 snRNA from irradiated particles was not immunoprecipitated with anti-SF3a66 antibodies (Fig. 3A, lanes 7 and 8, and data not shown). As the cognate SF3a120 peptide used to elute U2 snRNPs could hinder subsequent immunoprecipitation by anti-SF3a120 antibodies, to test for SF3a120-RNA interactions 17S U2 snRNPs were isolated using anti-SF3a66 antibodies as described previously (55). Importantly, identical cross-linking patterns were observed with 17S U2 snRNPs purified with both antibodies (data not shown) and none of the cross-links were immunoprecipitated with the anti-SF3a120 antibodies (data not shown). Thus, SF3a120 and SF3a66 either (i) do not contact the U2 snRNA directly or (ii) contact U2 but are in a conformation that does not favor the formation of UV-induced cross-links or their respective epitopes are not accessible, preventing immunoprecipitation. Taken together, these results suggest that SF3a contacts the U2 snRNA primarily via its 60-kDa subunit.

**SF3b14a/p14 contacts U2 snRNA close to the branch site-interacting region.** Anti-SF3b14a/p14 antibodies also precipitated a number of putative cross-links. Comparison of the primer extension patterns of U2 snRNAs recovered from the UV-irradiated 17S U2 snRNP before ("RNP"; Fig. 4, lanes 1) and after (lanes 5) immunoselection with SF3b14a/p14-specific antibodies revealed that the cross-link at G31 is clearly enriched in the immunoprecipitated fraction. Moreover, in contrast to the other immunoprecipitated species, this cross-link was not precipitated by any of the other antibodies tested. This indicates that G31, which is located only a few nucleotides from the pre-mRNA branch site-interacting region of U2, is contacted by SF3b14a/p14. These data are consistent with pre-

vious reports demonstrating that SF3b14a/p14 is directly cross-linked to the branch point adenosine in the context of the spliceosomal A complex where U2 is engaged in base-pairing interactions with the pre-mRNA's BPS (36).

**SF3b49 makes multiple contacts with the U2 snRNA.** The primer extension analysis of the cross-linked U2 snRNAs immunoprecipitated with anti-SF3b49 antibodies from the UV-irradiated native U2 particles generated a complex pattern (Fig. 3A and B, lanes 5 and 6). SF3b49-specific cross-links—i.e., those precipitated exclusively by anti-SF3b49 antibodies—were detected at the 5' end of U2 snRNA (Am1, Um2, and Ψ6) and in SLIIb (U74 and A75) (Fig. 3A and B, lanes 5). The most prominent cross-links precipitated by anti-SF3b49 antibodies were to nucleotides U18 (in loop I) and Ψ91-U92 (upstream of the Sm site), with the former being significantly enriched after immunoprecipitation with anti-SF3b49 antibodies (Fig. 3A and B [cf. lanes 1 and 5]). The Ψ91-U92 cross-links, as well as several other cross-links precipitated by anti-SF3b49 antibodies (e.g., U55 and Cm61 [cf. Fig. 4A, lanes 5 and 7]), were also precipitated by other antibodies, and thus they cannot be unequivocally identified. Others (i.e., U100 and U122) clearly represent cross-links with other U2 proteins, as U101 and A123 were the strongest reverse transcriptase stops observed after immunoprecipitation with anti-SmG and anti-SF3a60 antibodies, respectively (Fig. 3B, lane 7, and Fig. 4B, lane 7). Anti-SF3b155 and anti-SF3b145 antibodies precipitated only very small amounts of U2 snRNA from irradiated 17S U2 snRNPs; thus, a detailed analysis was difficult, as the respective primer extension patterns were very weak (data not shown). However, most discernible stops coincided with strong natural reverse transcriptase stops and no enrichment of any particular stop was observed after immunoprecipitation with these antibodies. Taken together, these data suggest that SF3b49 makes multiple contacts with the U2 snRNA, including its extreme 5' end and the loop of SLIIb (Fig. 5). Thus, it may be a major determinant for tethering SF3b to the U2 snRNP.

**SF3b49 interacts with the 5' end of U2 snRNA in reconstituted 17S U2 snRNPs.** To obtain independent evidence that SF3b49 contacts nucleotides at the very 5' end of the U2 snRNA, we performed UV cross-linking with in vitro-reconstituted U2 snRNPs. Previous reports indicated that modifications within the first 24 nucleotides of the human U2 snRNA are essential and sufficient for its activity in splicing (11). We thus prepared a chimeric U2 snRNA by ligating together a synthetic oligonucleotide,  $^{32}\text{P}$  labeled at its 5' end, that encompasses the 5' terminal 24 nucleotides of the U2 snRNA and contains all modifications (Fig. 6A), with an unmodified in vitro-transcribed RNA comprising the remaining part of U2. This chimeric U2 RNA was first incubated with purified total snRNP proteins to form 12S U2 snRNPs and later with HeLa nuclear extract specifically depleted of 12S U2 snRNPs to generate 17S U2 snRNPs (38). U2 snRNPs reconstituted in this way support pre-mRNA splicing in U2-depleted HeLa nuclear extract and thus are functionally active (11).

Reconstituted U2 particles were UV irradiated and treated with RNase T1 to generate a radiolabeled fragment comprising solely the first four nucleotides of U2, thereby allowing us to identify proteins cross-linked to nucleotides 1 to 4 of U2 snRNA. Gel analysis of the digested RNA revealed that more than 95% of the U2 RNA had been digested to completion (data not shown), with only a small amount of a partially digested fragment observed (Fig. 6B). A double band migrating at ~50 kDa on SDS-polyacrylamide gels was observed upon UV irradiation of 17S U2 snRNPs but not in the absence of UV (Fig. 6B [cf. lanes 1 and 2]). This cross-link was sensitive to proteinase K and was not observed with in vitro-reconstituted 12S U2 snRNPs or naked U2 snRNA (data not shown), suggesting that it was a cross-link between the SF3b49 protein and U2 snRNA. To determine the identity of the cross-linked protein, immunoprecipitations were performed with anti-SF3b49 and anti-SF3a60 antibodies after disruption of RNP complexes as described above. This cross-linked species was precipitated solely by anti-SF3b49 antibodies (Fig. 6B, lanes 3 to 6), confirming that it contains SF3b49. Note that the cross-link migrated faster and appeared as a single band after immunoprecipitation, most likely due to the presence of large amounts of heavy chain immunoglobulin G in the lanes. These results corroborate our cross-linking data obtained with native 17S U2 snRNPs, according to which SF3b49 could be cross-linked to nt Am1 and Um2 and thus provide independent evidence that the SF3b49 protein contacts the 5' end of the U2 snRNA.

**RNA-protein cross-linking in spliceosomal A and B complexes.** Next we addressed whether rearrangements occur in protein-RNA interactions within the U2 snRNP upon its integration into the spliceosomal A complex and/or upon the subsequent integration of the U4/U6.U5 tri-snRNP during B complex formation. For this purpose, spliceosomal complexes were purified using aptamer-tagged, adenovirus-derived MINX pre-mRNA and a tobramycin affinity selection method (18) followed by glycerol gradient centrifugation. Gradient fractions 11 to 12 were enriched in complex A (as evidenced by the nearly equimolar amounts of pre-mRNA and U1 and U2 snRNA), and fractions 15 to 16 contained predominantly complex B (as evidenced by the nearly equimolar amounts of pre-mRNA and U1, U2, U4, U5, and U6 snRNA) (Fig. 7A). B complexes were also isolated using an MS2 affinity purification method and a

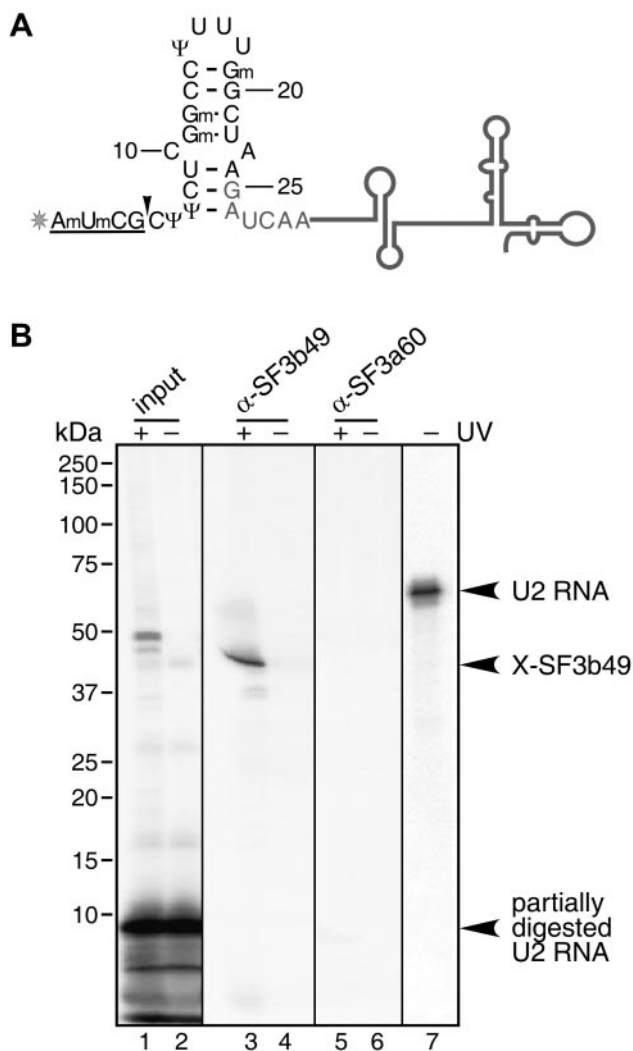


FIG. 6. Identification of proteins cross-linked to the 5' end of U2 snRNA in 17S U2 snRNPs reconstituted in vitro. (A) Schematic representation of the chimeric U2 snRNA prepared by ligation of a  $^{32}\text{P}$ -5'-end-labeled synthetic oligoribonucleotide, corresponding to the first 24 nucleotides of human U2 snRNA (shown in black), to in vitro-transcribed U2 encompassing nucleotides 25 to 187 (shown in gray). The radioactive label (asterisk) and the 5'-most RNase T1 cleavage site (arrowhead) are indicated. The 4-nt-long radioactive fragment of U2 generated by complete RNase T1 digestion of U2 snRNA is underlined. (B) 17S U2 snRNP particles were in vitro reconstituted with the chimeric U2 snRNA and subjected to UV irradiation (lanes 1, 3, and 5). U2 snRNPs in the even-numbered lanes and in lane 7 were not irradiated. All samples (except the lane 7 sample) were digested by RNase T1 and either directly analyzed by SDS-PAGE ("input"; lanes 1 and 2) or after immunoprecipitation with anti-SF3b49 (lanes 3 and 4) or anti-SF3a60 (lanes 5 and 6) antibodies. Protein-RNA cross-linked species were visualized by autoradiography. The positions of full-length U2, the SF3b49-U2 snRNA cross-link, and partially digested U2 snRNA are indicated by closed arrowheads on the right; note that the  $^{32}\text{P}$ -labeled 4-nt fragment has run out of the gel. The positions of molecular mass markers are shown on the left.

MINX pre-mRNA containing MS2 binding sites (9). After incubation with HeLa nuclear extract under splicing conditions, spliceosomal complexes were separated by glycerol gradient centrifugation, and the B complex peak was further pu-

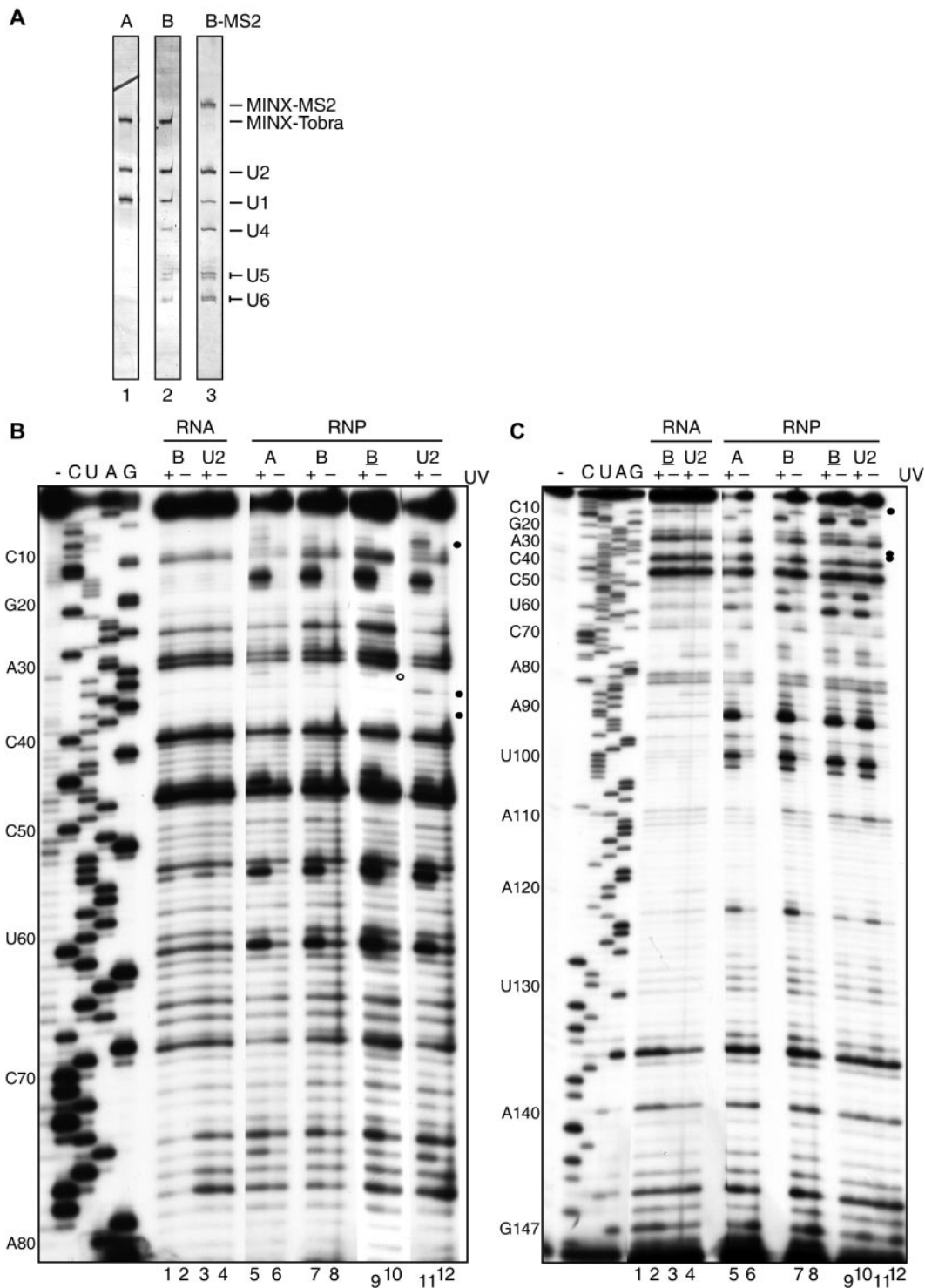


FIG. 7. Identification of U2 snRNA-protein cross-links in purified native spliceosomal A and B complexes. (A) RNA composition of affinity-purified spliceosomal complexes. RNA was isolated from tobramycin affinity-selected A (lane 1) or B (lane 2) complexes, or MS2 affinity-selected B complexes (lane 3), fractionated on a 7 M urea-10% polyacrylamide gel and visualized by silver staining. The position of the snRNAs or pre-mRNA is indicated on the right. (B and C) Primer extension analyses of UV-irradiated (lanes 1 and 3) or nonirradiated (lanes 2 and 4) naked U2 snRNA (RNA) isolated from purified spliceosomal B complexes or 17S U2 snRNPs (as indicated above each lane) or U2 snRNA extracted from UV-irradiated (lanes 5, 7, 9, and 11) or nonirradiated (lanes 6, 8, 10, and 12) affinity-purified A complex, B complex, or 17S U2 snRNPs (RNP), as indicated above each lane. B complexes isolated via the tobramycin affinity method are designated "B," whereas those isolated via MS2 affinity selection are labeled "B." Primers complementary to nt 97 to 117 (A) and 149 to 169 (B) were used, and primer extension products were visualized by autoradiography. Dideoxy sequencing markers were generated as described for Fig. 2. Nucleotide positions are shown on the left. RNA-protein cross-links present in isolated 17S U2 snRNPs but reduced in the purified spliceosomal A and B complexes (closed ovals) or cross-links observed in purified A and B complexes but not observed in free 17S U2 snRNPs (open oval) are indicated.

rified by binding to an amylose column and eluting with maltose. Native B complexes purified in this way also contained equimolar amounts of pre-mRNA and U1, U2, U4, U5, and U6 snRNA (Fig. 7A) and all major protein components (e.g., SF3a and SF3b) of the 17S U2 snRNP (J. Deckert, H. Urlaub, K. Hartmuth, and R. Lührmann, unpublished data).

A and B complexes were irradiated with 254 nm UV light, and cross-links to U2 snRNA were analyzed as described above. The overall U2 cross-linking patterns of gradient fractions 11 to 12 (A complex) and 15 to 16 (Tobra-B complex) as well as MS2 affinity-purified complex B were very similar to that observed for 17S U2 snRNP with the most prominent cross-links to nt 16, 55, 61, 92, 100, 102, and 122 (Fig. 7B and C, lanes 5 to 12). Thus, a global rearrangement in RNA-protein interactions within the U2 snRNP does not appear to occur during A and B complex assembly. However, clear differences in RNA-protein cross-links in the 5' part of U2 were observed. That is, cross-links to nt C8 and U9 (contacted by SF3a60 in U2 snRNPs), as well as to  $\Psi$ 34 and  $\Psi$ 37 (contacted by unidentified proteins), were greatly reduced in both A and B complexes compared to 17S U2 snRNP (Fig. 7B and C, closed circles). In addition, a novel cross-link to uridine 32 (open circle in Fig. 7B) appeared in both A and B complexes. Intriguingly, some of these changes appear in the functionally important regions of the U2 snRNA, which are known to interact with the BPS of the pre-mRNA earlier in the A complex and later with the U6 snRNA in complex B or B\* (activated spliceosomes) (reference 28; for a review, see reference 31). Immunoprecipitation of UV-irradiated, purified spliceosomal A and B complexes with anti-SF3a60 antibodies confirmed that SF3a60 contacted U122 in all complexes tested whereas C8 and U9 were efficiently cross-linked to SF3a60 only in 17S U2 snRNPs (data not shown). Due to the limited amount of material available for immunoprecipitations, it was not possible to identify the protein cross-linked to U32 of the U2 snRNA in the A and B spliceosomal complexes. Taken together, these results indicate that a rearrangement in the RNP architecture of the 5' end of the U2 snRNP occurs early during A complex formation, when U2 first stably associates with the BPS.

## DISCUSSION

Here we have investigated RNA-protein contact sites in the immunoaffinity-purified human 17S U2 snRNP via lead(II)-induced RNA cleavage and UV cross-linking studies. A number of cross-linked proteins, including SF3b49, SF3a60, and SF3b14a/p14, as well as their contact sites could be precisely assigned by performing cross-linking followed by immunoprecipitation. A similar analysis was carried out with affinity-purified spliceosomal A and B complexes. Data presented here provide much-needed information regarding the molecular architecture of the 17S U2 snRNP. They also provide insight into the dynamics of RNA-protein interactions within this spliceosomal subunit upon its stable integration into the A complex (i.e., prespliceosome) and during the subsequent conversion of the latter into the B complex (i.e., mature spliceosome).

**Multiple protein-RNA contacts within the 17S U2 snRNP.** Our lead(II)-induced RNA cleavage experiments provide initial evidence of how U2-associated proteins are positioned on

the U2 snRNA. Generally, the reactivity of most regions of the U2 snRNA was greatly reduced when 17S U2 snRNPs were probed compared to the results seen with naked RNA isolated from these particles, suggesting that the U2 snRNA makes multiple contacts with protein (Fig. 2). This is consistent with the large number of U2-associated proteins known to be associated with the 17S U2 snRNP (55) and previous studies revealing that most regions of the U2 snRNA within the U2 snRNP are resistant to nuclease treatment (25). Our UV cross-linking studies subsequently revealed numerous RNA-protein contacts throughout the U2 snRNA (Fig. 5), providing further evidence that the U2 snRNA is well protected by protein in the 17S U2 snRNP. As expected, nucleotides U100 to U105 located within the Sm site were completely protected from lead(II) cleavage, presumably due to the highly stable association of the Sm proteins with the Sm site. In agreement with previous structure probing and nuclease protection data, we also observed somewhat increased reactivity of RNA in the 17S U2 snRNP in those regions bordering the Sm site (17, 25). A decrease in the lead(II)-induced cleavage of the branch site-interacting region of the U2 snRNA was also observed, indicating that proteins contact the sugar-phosphate backbone of this region of U2. Such contacts would theoretically still allow for subsequent base-pairing interactions between U2 and the pre-mRNA BPS within the spliceosome and may even promote this interaction.

**Sm protein-Sm site interactions are conserved.** Using a combination of UV cross-linking and immunoprecipitation (44), we were able to assign a number of the cross-linking sites to specific proteins. Consistent with previous studies with purified U1 snRNPs and in vitro-reconstituted Sm core RNPs (20, 45), two major cross-linking sites involving the SmG and SmB proteins were observed within the Sm site of the immunoaffinity-purified U2 snRNP (Fig. 3). In particular, immunoprecipitation studies revealed contacts between U100 and U102 (i.e., the first and the third uridines of the Sm site) and the SmG and SmB/B' proteins, respectively. These data provide additional evidence that Sm protein-Sm site interactions are conserved among the spliceosomal snRNPs.

**SF3b14a/p14 is favorably positioned for its interaction with the BPS.** Interestingly, a contact site between SF3b14a/p14 and the U2 snRNA was mapped to G31, which is located just two nucleotides upstream of the branch site-interacting region (nt 33 to 38) of the U2 snRNA (Fig. 4). This region of U2 base pairs with the BPS of the pre-mRNA, resulting in a duplex in which the branch point adenosine is bulged out (35). SF3b14a/p14 was shown to contact this adenosine during early spliceosome assembly (i.e., in the A complex) and to remain attached to it through at least the first catalytic step of splicing (26, 36, 53). Due to its close contact with the BPS, it is suspected to play a crucial role in positioning the U2 snRNP on the pre-mRNA and in the first catalytic step of the splicing reaction. Our data indicate that early within the 17S U2 snRNP, SF3b14a/p14 is favorably positioned for its subsequent interaction with the branch point adenosine upon association of the U2 snRNP with the pre-mRNA's BPS.

SF3b14a/p14 is comprised predominantly of a single RRM, and RNA binding studies with isolated SF3b14a/p14 revealed that it possesses general nucleic acid binding activity but does not specifically recognize U2 snRNA or the BPS or their

duplex on its own (39). As high-affinity binding of SF3b14a/p14 to a U2 oligonucleotide comprising the branch site-interacting region was not observed in the aforementioned studies, it would appear that SF3b14a/p14 is not the main determinant for tethering other SF3b proteins to the U2 snRNP. Our cross-linking studies with purified A and B complexes did not provide clear information as to whether or not SF3b14a/p14 remains in contact with G31 of the U2 snRNA in spliceosomal complexes where it has been shown to contact the branch point adenosine. Thus, it is presently not clear whether SF3b14a/p14 contacts simultaneously both the pre-mRNA and the U2 snRNA within the spliceosome. Interestingly, a novel unidentified cross-link at U32 of U2 was observed in these complexes and could thus potentially be SF3b14a/p14. However, additional studies are required to clarify this point.

**SF3a60 contacts SLI and SLIII of the U2 snRNA.** Of the three proteins comprising SF3a, we identified cross-links between U2 snRNA and SF3a60 only, suggesting that this protein plays a key role in tethering SF3a to the U2 snRNP. In vitro studies indicate that SF3a incorporation into the U2 snRNP requires the prior assembly of a 15S U2 snRNP that contains SF3b and components of the 12S U2 snRNP (i.e., the Sm proteins and A'/B'') (25). In vitro reconstitution studies with purified, individual SF3a subunits indicate that SF3a60 (as well as the other SF3a proteins) can bind the 15S U2 snRNP on their own (30). Deletion analyses revealed that association of SF3a60 requires an intact zinc finger domain at its C terminus (30), which is the only conserved motif found in SF3a60. Zinc finger domains are known to bind nucleic acids; thus, it is tempting to speculate that this region of SF3a60 contacts the U2 snRNA. Taken together, our data indicate that the interaction of SF3a to form the 17S U2 snRNP is stabilized, at least in part, by direct U2 snRNA-SF3a60 contacts.

In addition to contacting the bulge in SLIII, SF3a60 made multiple contacts with the lower stem of SLI (Fig. 4). As UV-induced RNA-protein cross-links are generally not formed when nucleotides are engaged in base-pairing interactions, our results suggest that within the U2 snRNP, the lower part of SLI does not form. Likewise, previous structure-probing studies suggested that the base of stem I is unpaired in 17S U2 snRNPs (2). Formation of stem I is not essential, whereas its hyperstabilization has deleterious effects on splicing (56). Thus, SF3a60, together with other U2 proteins such as SF3b49, which was also cross-linked nearby, may help to maintain it in an unpaired conformation. This in turn likely facilitates the base-pairing interaction between this region of U2 and the U6 snRNA to form U2/U6 helix I and II, a crucial RNA structure at the catalytic core of the spliceosome (see below for detailed discussion).

**SF3b49 makes multiple contacts with the U2 snRNA.** Interestingly, SF3b49 was found to contact U2 snRNA at multiple sites, including its extreme 5' end and loops I and IIb. It contains two N-terminal RRM; thus, its domain structure suggests that it should possess RNA binding activity. SF3b49 was shown to play a role in tethering the U2 snRNP to the BPS during spliceosomal A complex assembly, contacting the pre-mRNA just upstream of the BPS (15) and interacting with another component of the U2 snRNP, the SF3b145 protein (6). The *Caenorhabditis elegans* homologue of SF3b49 was shown to bind RNA in vitro primarily via its RRM2 (43). In

yeast, the protein-protein interaction site of HSH49 and Cus1p, the yeast homologues of the human SF3b49 and SF3b145 proteins, respectively (49), was mapped to the first RRM of HSH49. Further mutational analyses indicated that the RNA and protein binding surfaces of the RRM1 of HSH49 are most likely distinct and that both RRMs are required for viability in yeast (22). Based on the detection of multiple cross-links involving SF3b49, it is likely that the observed cross-linking pattern (involving different regions of the U2 snRNA) would require the contribution of both RRMs. However, as cross-linking implies close contact and not necessarily binding per se, regions other than SF3b49's RRMs could also be cross-linked.

The interactions of SF3b49 and SF3a60 with the 5' end of the U2 snRNA (including SLI) described here might be of primary importance for the integrity of 17S U2 snRNPs. That is, it was observed previously that removal of 10 to 15 nucleotides from the 5' end of U2 snRNA results in a loss of the majority of proteins, changing the sedimentation value of the particle to 10S to 12S (2). Thus, SF3b49 and SF3a60 could potentially play a crucial role in tethering the SF3a/b complexes to U2 snRNP. Within the spliceosome, SF3b49, as well as SF3a60, contacts a relatively short region (about 25 nt) of the pre-mRNA upstream of the BPS (6, 15, 40). As with SF3b14a/p14, it is presently not clear whether these proteins contact simultaneously both the pre-mRNA and the U2 snRNA in spliceosomal complexes. However, as the U2 snRNA cross-linking pattern in purified A and B complexes was nearly identical to that in purified 17S U2 snRNPs (with notable exceptions at the 5' end of U2; see below), several SF3b49 and SF3a60 contacts with the U2 snRNA (e.g., at nucleotides 74, 75, and 122) appear to remain unchanged. Thus, it is likely that these proteins simultaneously contact the U2 snRNA and the pre-mRNA in the vicinity of the BPS.

As SF3b is also a component of the U11/U12 snRNP, our data may provide first insights into how SF3b is incorporated into this snRNP particle. That is, it is likely that SF3b49 also contacts the U12 snRNA within the U11/U12 snRNP. As the sequences of U12 and U2 are essentially unrelated but the general structures of their 5' halves are similar, SF3b49 could be envisioned to bind in a sequence-independent manner to analogous regions of the U12 snRNA. However, additional studies (i.e., UV cross-linking of purified U11/U12 snRNPs) are clearly required to answer this question.

**Additional proteins likely contact the U2 snRNA.** The protein moiety of a number of U2 snRNA-protein cross-links could not be identified, due to lack of antibodies or the inaccessibility of the epitope recognized by the antibodies at hand (Fig. 5). Thus, additional U2-associated proteins appear to contact the U2 snRNA. Furthermore, some RNA-protein interactions may have escaped detection, as only those in a conformation favorable for UV cross-linking would be observed. Indeed, previous studies suggested that SF3b145 contacts the U2 snRNA. The cross-links to nucleotides Cm40 and U46, as well as those to SLIIa, might be due to interactions with SF3b145, as several genetic studies performed with yeast linked this protein to these regions of the U2 snRNA (49, 57). Likewise, Prp9-Prp11-Prp21 (the yeast homologues of SF3a60, SF3a66, and SF3a120, respectively) and Prp5 were found to genetically interact with nucleotides just upstream of SLIIa, as well as with SLIIa and SLIIb, suggesting that these factors

might bind to these regions of U2 (37, 48, 57). Finally, on the basis of the U2 model presented by Krämer et al. (25) (see below), the cross-links in the loop of SLIII might involve SF3a120 and/or SF3a66.

**A more compact RNP structure for the 17S U2 snRNP?** Previous biochemical and electron microscopy studies (2, 25) suggested a model of 17S U2 snRNP organization in which SF3b proteins interact with the 5' half of the U2 snRNA whereas the Sm proteins, SF3a and U2-A'/U2-B'', bind to its 3' half and form a second domain of the U2 snRNP. Consistent with this model, two SF3b subunits (SF3b49 and SF3b14a/p14) were cross-linked to the 5' part of the U2 snRNA (i.e., within nt 1 to 31) whereas one of the contact sites of SF3a60 was mapped to the bulge in SLIII (Fig. 3 and 4). Intriguingly, a second site of interaction with SF3a60 was found at the base of SLI, indicating that SF3a60 spans the 5' and 3' halves of the U2 snRNA. Thus, the 17S U2 snRNP might have a more compact structure than previously thought (2, 25). Indeed, electron microscopy imaging of the 17S U2 particles used in this study revealed that they predominantly have a globular shape (B. Sander, M. M. Golas, C. L. Will, B. Kastner, H. Stark, and R. Lührmann, unpublished data) rather than two smaller domains connected with a thin filament (i.e., a dumbbell shape) as previously reported (2, 25). This difference in appearance most likely arises from the different purification conditions used in each study and suggests that some of the interactions within the 17S U2 snRNP are not particularly stable.

**Evidence for U2 snRNP remodeling upon its stable integration into the spliceosome.** Examination of U2 snRNA-protein interactions in purified spliceosomal A and B complexes revealed that the RNP structure involving the 5' end of the U2 snRNA undergoes a conformational change during spliceosome assembly. That is, cross-links to nucleotides 8 and 9 (SLI) and to nucleotides 34 and 37 (branch site-interacting region) were significantly reduced in both spliceosomal complexes compared to the results seen with the free 17S U2 snRNP (Fig. 7). In contrast, enhanced cross-link formation was observed at nucleotide 32 in spliceosomal complexes. The observed changes were quantitative in nature (e.g., residual cross-linking to nt 8, 9, 34, and 37 was consistently observed), suggesting that the complexes analyzed may be structurally heterogeneous or contain small amounts of contaminating 17S U2 snRNPs. Nonetheless, our data indicate that the U2 snRNP has already been remodeled at the time of its stable interaction with the BPS of the pre-mRNA.

Interestingly, the 5' end of the U2 snRNA is involved in an extensive RNA network, formed by U2, U6, and the pre-mRNA, that is essential for splicing (reviewed in reference 31). While the U2 snRNA-BPS base-pairing interaction is known to be first established during A complex formation (i.e., in the prespliceosome), U2-U6 interactions occur after tri-snRNP addition (after B complex formation). However, it is presently not clear whether these interactions have already been established in the B complex or occur only at the time of spliceosome activation (for a recent discussion, see reference 28). At present, three different U2/U6 base-pairing interactions have been reported: helix I, consisting of helix Ia and Ib separated by two unpaired adenosines of U2 (27), helix II (19), and helix III (42).

Intriguingly, the observed changes in the U2 snRNA cross-linking pattern in spliceosomal complexes involve protein contacts with nucleotides of U2 forming U2/U6 helix II (C8 and U9) and nucleotides upstream (U32) or within the branch point helix ( $\Psi$ 34 and  $\Psi$ 37). Our finding that SF3a60 is bound to nucleotides 8 and 9 of the U2 snRNA and that these contacts are significantly reduced upon association of U2 with the BPS in the A complex indicates that the RNP rearrangements involve SF3a60. Immunoprecipitations with anti-SF3a60 antibodies of the A and B complexes after UV irradiation showed that this protein does not completely leave the U2 snRNP (data not shown); thus, it likely remains attached to the bulge in SLIII in spliceosomal complexes. As UV-induced RNA-protein cross-links are typically not formed when nucleotides are engaged in base-pairing interactions, it is currently not clear whether the unknown protein(s) contacting  $\Psi$ 34 and  $\Psi$ 37 (which are base paired already in the A complex) are displaced from the U2 snRNA or whether the relative protein-RNA orientation was changed due to base-pairing interactions such that cross-linking is prevented. Likewise, the loss of the C8 and U9 cross-links in the purified B complexes could be due to the formation of the U2/U6 helix II, which involves these nucleotides. However, as the cross-links to C8-U9 disappear and the cross-link to U32 has already appeared in the A complex, when no U6 is present (18), these RNP rearrangements occur early on and are not a consequence of U2/U6 helix formation. Indeed, based on their location, one or more of these rearrangements may facilitate or be a prerequisite for subsequently establishing U2/U6 base-pairing interactions. Even though the identity of the protein(s) cross-linked to U32,  $\Psi$ 34, and  $\Psi$ 37 has not been determined, it is tempting to speculate that it is SF3b14a/p14, which might "move" towards the branch point adenosine, switching from G31 in the isolated 17S U2 snRNP to U32 in the spliceosome.

#### ACKNOWLEDGMENTS

We are grateful to Gabi Heyne, Thomas Conrad, Hossein Kohansal, and Irene Öchsner for excellent technical assistance. We thank Henning Urlaub for helpful discussions and Gizem Dönmez for kindly providing native snRNP proteins and synthetic RNA oligonucleotides for U2 snRNP reconstitutions.

This work was supported by grants from the DFG Forschergruppe, Fonds der Chemischen Industrie, and the Ernst-Jung Stiftung to R.L.

#### REFERENCES

1. Ares, M., Jr., and A. H. Igel. 1990. Lethal and temperature-sensitive mutations and their suppressors identify an essential structural element in U2 small nuclear RNA. *Genes Dev.* **4**:2132–2145.
2. Behrens, S. E., K. Tyc, B. Kastner, J. Reichelt, and R. Lührmann. 1993. Small nuclear ribonucleoprotein (RNP) U2 contains numerous additional proteins and has a bipartite RNP structure under splicing conditions. *Mol. Cell. Biol.* **13**:307–319.
3. Brosi, R., K. Gröning, S. E. Behrens, R. Lührmann, and A. Krämer. 1993. Interaction of mammalian splicing factor SF3a with U2 snRNP and relation of its 60-kD subunit to yeast PRP9. *Science* **262**:102–105.
4. Brunel, C., and P. Romby. 2000. Probing RNA structure and RNA-ligand complexes with chemical probes. *Methods Enzymol.* **318**:3–21.
5. Caspary, F., A. Shevchenko, M. Wilm, and B. Séraphin. 1999. Partial purification of the yeast U2 snRNP reveals a novel yeast pre-mRNA splicing factor required for pre-spliceosome assembly. *EMBO J.* **18**:3463–3474.
6. Champion-Arnaud, P., and R. Reed. 1994. The prespliceosome components SAP 49 and SAP 145 interact in a complex implicated in tethering U2 snRNP to the branch site. *Genes Dev.* **8**:1974–1983.
7. Chiara, M. D., P. Champion-Arnaud, M. Buvoli, B. Nadal-Ginard, and R. Reed. 1994. Specific protein-protein interactions between the essential mammalian spliceosome-associated proteins SAP 61 and SAP 114. *Proc. Natl. Acad. Sci. USA* **91**:6403–6407.

8. Das, B. K., L. Xia, L. Palandjian, O. Gozani, Y. Chyung, and R. Reed. 1999. Characterization of a protein complex containing spliceosomal proteins SAPs 49, 130, 145, and 155. *Mol. Cell. Biol.* **19**:6796–6802.
9. Das, R., Z. Zhou, and R. Reed. 2000. Functional association of U2 snRNP with the ATP-independent spliceosomal complex E. *Mol. Cell* **5**:779–787.
10. Dignam, J. D., R. M. Lebovitz, and R. G. Roeder. 1983. Accurate transcription initiation by RNA polymerase II in a soluble extract from isolated mammalian nuclei. *Nucleic Acids Res.* **11**:1475–1489.
11. Dönmez, G., K. Hartmuth, and R. Lührmann. 2004. Modified nucleotides at the 5' end of human U2 snRNA are required for spliceosomal E-complex formation. *RNA* **10**:1925–1933.
12. Dziembowski, A., A. P. Ventura, B. Rutz, F. Caspary, C. Faux, F. Halgand, O. Laprèvote, and B. Séraphin. 2004. Proteomic analysis identifies a new complex required for nuclear pre-mRNA retention and splicing. *EMBO J.* **23**:4847–4856.
13. Golas, M. M., B. Sander, C. L. Will, R. Lührmann, and H. Stark. 2003. Molecular architecture of the multiprotein splicing factor SF3b. *Science* **300**:980–984.
14. Golas, M. M., B. Sander, C. L. Will, R. Lührmann, and H. Stark. 2005. Major conformational change in the complex SF3b upon integration into the spliceosomal U11/U12 di-snRNP as revealed by electron cryomicroscopy. *Mol. Cell* **17**:869–883.
15. Gozani, O., R. Feld, and R. Reed. 1996. Evidence that sequence-independent binding of highly conserved U2 snRNP proteins upstream of the branch site is required for assembly of spliceosomal complex A. *Genes Dev.* **10**:233–243.
16. Gozani, O., J. Potashkin, and R. Reed. 1998. A potential role for U2AF-SAP 155 interactions in recruiting U2 snRNP to the branch site. *Mol. Cell. Biol.* **18**:4752–4760.
17. Hartmuth, K., V. A. Raker, J. Huber, C. Branlant, and R. Lührmann. 1999. An unusual chemical reactivity of Sm site adenosines strongly correlates with proper assembly of core U snRNP particles. *J. Mol. Biol.* **285**:133–147.
18. Hartmuth, K., H. Urlaub, H.-P. Vornlocher, C. L. Will, M. Gentzel, M. Wilm, and R. Lührmann. 2002. Protein composition of human prespliceosomes isolated by a tobramycin affinity-selection method. *Proc. Natl. Acad. Sci. USA* **99**:16719–16724.
19. Hausner, T. P., L. M. Giglio, and A. M. Weiner. 1990. Evidence for base-pairing between mammalian U2 and U6 small nuclear ribonucleoprotein particles. *Genes Dev.* **4**:2146–2156.
20. Heinrichs, V., W. Hackl, and R. Lührmann. 1992. Direct binding of small nuclear ribonucleoprotein G to the Sm site of small nuclear RNA. Ultraviolet light cross-linking of protein G to the AAU stretch within the Sm site (AAUUUGUGG) of U1 small nuclear ribonucleoprotein reconstituted in vitro. *J. Mol. Biol.* **227**:15–28.
21. Hermann, H., P. Fabrizio, V. A. Raker, K. Foulaki, H. Hornig, H. Brahm, and R. Lührmann. 1995. snRNP Sm proteins share two evolutionarily conserved sequence motifs which are involved in Sm protein-protein interactions. *EMBO J.* **14**:2076–2088.
22. Igel, H., S. Wells, R. Perriman, and M. Ares, Jr. 1998. Conservation of structure and subunit interactions in yeast homologues of splicing factor 3b (SF3b) subunits. *RNA* **4**:1–10.
23. Kambach, C., S. Walke, R. Young, J. M. Avis, E. de la Fortelle, V. A. Raker, R. Lührmann, J. Li, and K. Nagai. 1999. Crystal structures of two Sm protein complexes and their implications for the assembly of the spliceosomal snRNPs. *Cell* **96**:375–387.
24. Krämer, A., F. Mulhauser, C. Wersig, K. Gröning, and G. Bilbe. 1995. Mammalian splicing factor SF3a120 represents a new member of the SURP family of proteins and is homologous to the essential splicing factor PRP21p of *Saccharomyces cerevisiae*. *RNA* **1**:260–272.
25. Krämer, A., P. Grüter, K. Gröning, and B. Kastner. 1999. Combined biochemical and electron microscopic analyses reveal the architecture of the mammalian U2 snRNP. *J. Cell Biol.* **145**:1355–1368.
26. MacMillan, A. M., C. C. Query, C. R. Allerson, S. Chen, G. L. Verdine, and P. A. Sharp. 1994. Dynamic association of proteins with the pre-mRNA branch region. *Genes Dev.* **8**:3008–3020.
27. Madhani, H. D., and C. Guthrie. 1992. A novel base-pairing interaction between U2 and U6 snRNAs suggests a mechanism for the catalytic activation of the spliceosome. *Cell* **71**:803–817.
28. Makarova, O. V., E. M. Makarov, H. Urlaub, C. L. Will, M. Gentzel, M. Wilm, and R. Lührmann. 2004. A subset of human 35S U5 proteins, including Prp19, function prior to catalytic step 1 of splicing. *EMBO J.* **23**:2381–2391.
29. Moore, M. J., and P. A. Sharp. 1992. Site-specific modification of pre-mRNA: the 2'-hydroxyl groups at the splice sites. *Science* **256**:992–997.
30. Nestic, D., and A. Krämer. 2001. Domains in human splicing factors SF3a60 and SF3a66 required for binding to SF3a120, assembly of the 17S U2 snRNP, and prespliceosome formation. *Mol. Cell. Biol.* **21**:6406–6417.
31. Nilsen, T. W. 1998. RNA-RNA interactions in nuclear pre-mRNA splicing, p. 279–307. *In* R. W. Simons and M. Grunberg-Manago (ed.), *RNA structure and function*. Cold Spring Harbor Laboratory Press, Cold Spring Harbor, N.Y.
32. Patel, A. A., and J. A. Steitz. 2003. Splicing double: insights from the second spliceosome. *Nat. Rev. Mol. Cell Biol.* **4**:960–970.
33. Price, S. R., P. R. Evans, and K. Nagai. 1998. Crystal structure of the spliceosomal U2B<sup>+</sup>-U2A<sup>+</sup> protein complex bound to a fragment of U2 small nuclear RNA. *Nature* **394**:645–650.
34. Pruijn, G. J. M., F. Schoute, J. P. H. Thijssen, R. J. T. Smeenk, and W. J. van Venrooij. 1997. Mapping of SLE-specific Sm B cell epitopes using murine monoclonal antibodies. *J. Autoimmun.* **10**:127–136.
35. Query, C. C., M. J. Moore, and P. A. Sharp. 1994. Branch nucleophile selection in pre-mRNA splicing: evidence for the bulged duplex model. *Genes Dev.* **8**:587–597.
36. Query, C. C., S. A. Strobel, and P. A. Sharp. 1996. Three recognition events at the branch-site adenine. *EMBO J.* **15**:1392–1402.
37. Ruby, S. W., T. H. Chang, and J. Abelson. 1993. Four yeast spliceosomal proteins (PRP5, PRP9, PRP11, and PRP21) interact to promote U2 snRNP binding to pre-mRNA. *Genes Dev.* **7**:1909–1925.
38. Ségault, V., C. L. Will, B. S. Sproat, and R. Lührmann. 1995. In vitro reconstitution of mammalian U2 and U5 snRNPs active in splicing: Sm proteins are functionally interchangeable and are essential for the formation of functional U2 and U5 snRNPs. *EMBO J.* **14**:4010–4021.
39. Spadaccini, R., U. Reidt, O. Dybkov, C. L. Will, R. Frank, G. Stier, L. Corsini, M. C. Wahl, R. Lührmann, and M. Sattler. Biochemical and NMR analyses of an SF3b155-p14-U2AF-RNA interaction network involved in branch point definition during pre-mRNA splicing. *RNA*, in press.
40. Staknis, D., and R. Reed. 1994. Direct interactions between pre-mRNA and six U2 small nuclear ribonucleoproteins during spliceosome assembly. *Mol. Cell. Biol.* **14**:2994–3005.
41. Staley, J. P., and C. Guthrie. 1998. Mechanical devices of the spliceosome: motors, clocks, springs, and things. *Cell* **92**:315–326.
42. Sun, J. S., and J. L. Manley. 1995. A novel U2-U6 snRNA structure is necessary for mammalian mRNA splicing. *Genes Dev.* **9**:843–854.
43. Tanaka, Y., A. Ohta, K. Terashima, and H. Sakamoto. 1997. Polycistronic expression and RNA-binding specificity of the *C. elegans* homologue of the spliceosome-associated protein SAP49. *J. Biochem. (Tokyo)* **121**:739–745.
44. Urlaub, H., K. Hartmuth, S. Kostka, G. Grelle, and R. Lührmann. 2000. A general approach for identification of RNA-protein cross-linking sites within native human spliceosomal small nuclear ribonucleoproteins (snRNPs). Analysis of RNA-protein contacts in native U1 and U4/U6.U5 snRNPs. *J. Biol. Chem.* **275**:41458–41468.
45. Urlaub, H., V. A. Raker, S. Kostka, and R. Lührmann. 2001. Sm protein-Sm site RNA interactions within the inner ring of the spliceosomal snRNP core structure. *EMBO J.* **20**:187–196.
46. Varani, G., and K. Nagai. 1998. RNA recognition by RNP proteins during RNA processing. *Annu. Rev. Biophys. Biomol. Struct.* **27**:407–445.
47. Wang, Q., and B. C. Rymond. 2003. Rds3p is required for stable U2 snRNP recruitment to the splicing apparatus. *Mol. Cell. Biol.* **23**:7339–7349.
48. Wells, S. E., and M. Ares, Jr. 1994. Interactions between highly conserved U2 small nuclear RNA structures and Prp5p, Prp9p, Prp11p, and Prp21p proteins are required to ensure integrity of the U2 small nuclear ribonucleoprotein in *Saccharomyces cerevisiae*. *Mol. Cell. Biol.* **14**:6337–6349.
49. Wells, S. E., M. Neville, M. Haynes, J. Wang, H. Igel, and M. Ares, Jr. 1996. CUS1, a suppressor of cold-sensitive U2 snRNA mutations, is a novel yeast splicing factor homologous to human SAP 145. *Genes Dev.* **10**:220–232.
50. Will, C. L., and R. Lührmann. 2001. Spliceosomal UsnRNP biogenesis, structure and function. *Curr. Opin. Cell Biol.* **13**:290–301.
51. Will, C. L., and R. Lührmann. 2006. Spliceosome structure and function, p. 369–400. *In* R. F. Gesteland, T. R. Cech, and J. F. Atkins (ed.), *The RNA world*, 3<sup>rd</sup> ed. Cold Spring Harbor Laboratory Press, Cold Spring Harbor, New York.
52. Will, C. L., B. Kastner, and R. Lührmann. 1994. Analysis of ribonucleoprotein interactions, p. 141–177. *In* S. J. Higgins and B. D. Hames (ed.), *RNA processing: a practical approach*, vol. 1. IRL Press, Oxford, United Kingdom.
53. Will, C. L., C. Schneider, A. M. MacMillan, N. F. Katopodis, G. Neubauer, M. Wilm, R. Lührmann, and C. C. Query. 2001. A novel U2 and U11/U12 snRNP protein that associates with the pre-mRNA branch site. *EMBO J.* **20**:4536–4546.
54. Will, C. L., C. Schneider, R. Reed, and R. Lührmann. 1999. Identification of both shared and distinct proteins in the major and minor spliceosomes. *Science* **284**:2003–2005.
55. Will, C. L., H. Urlaub, T. Achsel, M. Gentzel, M. Wilm, and R. Lührmann. 2002. Characterization of novel SF3b and 17S U2 snRNP proteins, including a human Prp5p homologue and an SF3b DEAD-box protein. *EMBO J.* **21**:4978.
56. Wu, J., and J. L. Manley. 1992. Multiple functional domains of human U2 small nuclear RNA: strengthening conserved stem I can block splicing. *Mol. Cell. Biol.* **12**:5464–5473.
57. Yan, D., and M. Ares, Jr. 1996. Invariant U2 RNA sequences bordering the branchpoint recognition region are essential for interaction with yeast SF3a and SF3b subunits. *Mol. Cell. Biol.* **16**:818–828.